A printable supercapacitor as a storage unit in an RF energy harvester

Suvi Lehtimäki[a,*], Miao Li[a], Jarno Salomaa[b], Juho Pörhönen[a], Antti Kalanti[b], Sampo Tuukkanen[a], Petri Heljo[a], Kari Halonen[b], Donald Lupo[a]

[a] *Tampere University of Technology, Department of Electronics and Communications Engineering, Korkeakoulunkatu 3, FI-33720, Tampere, Finland*
[b] *Aalto University, School of Electrical Engineering, Department of Micro- and Nanosciences, Otakaari 5 A, FI-02150, Espoo, Finland*

Abstract

We report the fabrication of a supercapacitor on a plastic substrate with mass-production-compatible methods and its characterisation using galvanostatic and voltammetric methods. The supercapacitor is prepared in ambient conditions using activated carbon and an aqueous, non-acidic electrolyte. The obtained capacitances are 450 mF and 210 mF for device sizes of 4 cm^2 and 2 cm^2, respectively. Additionally, we demonstrate the utilisation of the supercapacitor in an autonomous energy harvesting and storage system. The RF energy harvester comprises a printed loop antenna and an organic rectifying diode operating at 13.56 MHz frequency. The harvested energy is stored in two supercapacitors connected in series to increase the maximum voltage. In order to power a device such as a sensor or a small indicator display, voltage regulation is needed: this is provided by a voltage regulator ASIC (application specific integrated circuit). We demonstrate the ability of the harvester storage unit to power the regulator for hours with a constant output. The effect of supercapacitor charging time on the steady output duration is also discussed, as a slower charging due to weaker antenna coupling is found to have a significant effect on the output from the supercapacitor.

Keywords:
Supercapacitor, Ultracapacitor, Electric double layer capacitor, Energy harvesting, Autonomous power source

1. Introduction

Energy harvesting from ambient sources such as light, radio frequency (RF) fields or kinetic energy provides an opportunity for building wireless, autonomous systems that can be used, for example, in ambient sensory networks or intelligent packaging [1–3]. Incorporating such "intelligence" on large areas cost-effectively, i.e. roll-to-roll, calls for a new way of producing the systems needed. Printed and organic electronics offers a promising manufacturing method, where flexible, lightweight and even transparent electronic devices are possible [4–6].

An autonomous harvesting system needs a backup energy storage for periods where the primary energy source is unavailable [2], such as during the night when using solar cells, or when RF fields are not present when using RF harvesters. Supercapacitors, also called ultracapacitors or electric double layer capacitors (EDLC), are an alternative to batteries as energy storage devices, offering a higher peak power capability and a longer cycle lifetime [7].

The operation of supercapacitors is based on the electrostatic aggregation of electrolyte ions on a charged electrode surface, without significant chemical reactions. Using a high surface area electrode material, such as activated carbon, very high capacitances can be reached [7]. A limitation of supercapacitors is their operation voltage range, which is constrained by the electrochemistry of the materials. In water-based electrolytes, the voltage is limited to only about 1 V, whereas with organic electrolytes 2–3 V is attainable [8]. However, aqueous electrolytes offer smaller equivalent series resistance and higher specific capacitance than organic electrolytes [8]. They are also readily disposable and their production is less expensive, which is in many applications more advantageous than higher operation voltage. The voltage range can also be increased by connecting supercapacitors in series.

Printed supercapacitors on a paperboard substrate have previously been demonstrated using disposable, non-toxic materials [9]. RF harvesters, comprising an antenna and a rectifier circuit, can also be fabricated with printing methods [10]. With the development of organic devices, complete printed circuits will in the future be possible. Integration of printed and traditional components is a stepping stone for the research into fully printed systems. For example, valuable insight into the charging and discharging behaviour of the printed energy storage device can be obtained.

In this study, printed, aqueous supercapacitors are connected to a printed RF harvester [10] and a voltage control application-specific integrated circuit (ASIC) [11]. This harvesting circuit provides up to 10 hours of steady output when the RF field is not present. The capacitance of the supercapacitor can easily be tailored for the requirements of the application by selecting the supercapacitor geometrical area appropriately.

*Corresponding author. Tel.: +358 408490623.
Email address: suvi.lehtimaki@tut.fi (Suvi Lehtimäki)

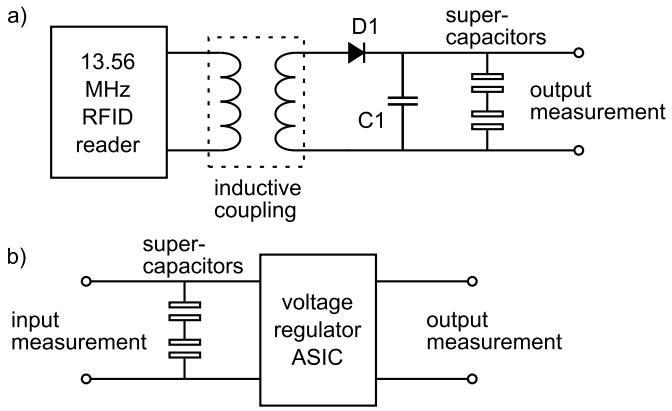

Figure 1: Schematics of the supercapacitor a) harvesting and b) output measurement circuits. Diode D1 and capacitor C1 form the rectifier, which charges the supercapacitor.

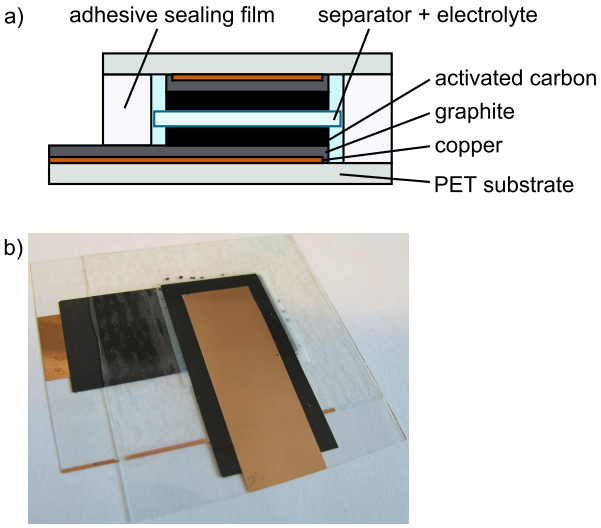

Figure 2: a) Structure of the assembled supercapacitor and b) photograph of a 4 cm^2 supercapacitor sample.

2. Experimental

Printed components were fabricated on poly(ethylene terephthalate) (PET) substrates (Melinex ST506 from Dupont Teijin Films). A commercial RFID reader was used to induce an AC voltage in a printed antenna. A printed rectifier circuit composed of an organic diode [12] and a printed capacitor rectifies the input from the antenna, and charges the supercapacitor. The charged supercapacitor provides an input for the voltage regulator ASIC, which is connected to a 1 MΩ load at its output. The measurement setup is depicted in Fig. 1.

2.1. Supercapacitor fabrication

The supercapacitors were prepared by sandwiching two electrodes together with an electrolyte and separator in between. The structure is depicted in Fig. 2. The supercapacitors were fabricated in two sizes: 2 cm^2 and 4 cm^2. A 100 nm thick copper layer was vacuum evaporated onto the PET through a shadow mask. Two layers of conductive graphite ink (Electrodag PC407C from Acheson Industries Ltd.) were blade-coated on top of the copper and both layers were subsequently cured at 120 °C for 5 min, yielding a 50 µm thick layer. The width of the graphite electrodes was 2.0 cm in the larger samples and 1.4 cm in the smaller samples. As the graphite layer was needed to protect the copper layer from coming into contact with the electrolyte, the copper electrode width was slightly smaller than the graphite.

The active layer was prepared from Norit DLC Super 50 activated carbon with carboxymethyl cellulose (CMC, Sigma Aldrich) as binder. The activated carbon and the polymer were dispersed in deionized water with the ratio Norit/CMC/H_2O 1.9/0.1/36 by weight. The activated carbon ink layer was blade-coated on the graphite using a plastic mask for patterning. The active layer was dried on a hotplate at 60 °C for a few minutes until the ink appeared dried. The mass of activated carbon deposited on the electrodes was on average 2.2 g/cm^2. The activated carbon mass was determined by weighing the substrate before and after deposition.

Supercapacitors were assembled with a TF4050 paper separator (Nippon Kodoshi Corporation) and 4.1 mol/l LiCl aqueous electrolyte. The high electrolyte concentration was selected to ensure an excess of ions such that the risk for electrolyte starvation and additional internal resistance is removed [13]. The electrodes and separator were sandwiched together with the electrolyte and sealed with an adhesive film (UPM Raflatac). The assembly was done with the electrodes at 90°angle with respect to each other, forming a square shape supercapacitor at the electrode overlap area.

2.2. Supercapacitor characterization

The supercapacitor properties were measured using a Zennium Electrochemical Workstation (Zahner Elektrik GmbH, Germany) in the two-electrode configuration. Cyclic voltammetry from 0 V to 0.9 V was used to get a qualitative measure of the supercapacitors. The voltage sweep rate was 50 mV/s.

Galvanostatic discharging measurements were performed according to international standard IEC 62391-1:2006, Class 3 [14]. The supercapacitors were charged to 0.9 V in 1 min and held at this potential for 5 min. The capacitance was calculated from the voltage decrease rate with a 1.60 mA discharge current for the larger samples and 725 A for the smaller samples. The equivalent series resistance (ESR) was calculated from the initial IR drop of the discharging with a 16.0 mA current for the larger samples and 7.25 mA for the smaller samples.

2.3. Harvester architecture

The all-printed harvester consisted of an antenna and a half-wave rectifier comprising an organic diode and a capacitor. The loop antenna was inkjet printed with a conductive Ag nanoparticle ink (Harima NPS-JL Silver NanoPaste) and a dielectric (SunTronic Jettable insulator U5388) for the loop cross-over. The Ag ink was sintered at 150 °C for 1 h. The dielectric strip was cured by UV light and by additional curing at 150 °C for

30 min, after which the loop cross-over was printed with the same Ag ink as the antenna.

The organic diode was fabricated on a separate substrate, where the Cu anode was evaporated and patterned using a wet-etching process on a roll-to-roll basis. The semiconductor poly(triarylamine) as well as the top Ag anode were gravure printed. The process is described in more detail in [12]. The rectifier capacitor was also printed on a similar pre-patterned Cu-coated substrate. The dielectric was gravure printed poly(methyl metacrylate) (20 % solution in ethyl acetate and toluene, 1:1) cured at 80 °C for 5 min. The top electrode was gravure printed using Ag flake ink (Acheson PM460A) and cured at 80 °C for 5 min. The capacitance was 1.5 nF at 13.56 MHz. The diode and capacitor were integrated on the antenna substrate using the Ag flake ink.

2.4. Measurement setup

Two similar supercapacitors were connected in series. The supercapacitors were charged by connecting them to the harvester, after which they were connected to the ASIC for the output measurement.

The harvester antenna was placed above a 13.56 MHz reader antenna (i-scan® HF long range reader ID ISC.LR200 from OBID) and the position of the harvester was adjusted vertically between 5.5 cm and 6.0 cm. The input from the antenna in these two cases was measured using an oscilloscope (Tektronix DPO4104) with a 10X voltage probe when only the rectifier was connected to the antenna. The output from the rectifier was measured similarly before the supercapacitor was connected.

The series supercapacitors were charged to 1.8 V with the harvester, and the voltage over the supercapacitors was measured with the oscilloscope through a 10X voltage probe. The oscilloscope was controlled with a LabVIEW software (National Instruments). The charging was stopped by removing the reader antenna when the voltage over the supercapacitor reached the target value.

For the discharging, the supercapacitor assembly was connected to the ASIC, and the ASIC output voltage measured over a [buffered (how do we describe this?)] 1 MΩ load. The voltages were measured with the oscilloscope.

3. Results and discussion

3.1. Supercapacitor properties

Cyclic voltammograms of the supercapacitors of two sizes using a sweep rate of 50 mV/s are shown in Fig. 3a. The rectangular shape indicates good capacitive behaviour [15, chap. 2]. The capacitances and ESRs were determined from the galvanostatic discharge measurements (Fig. 3 b and c). The capacitances were approximately 450 mF and 210 mF in the 4 cm^2 and 2 cm^2 supercapacitors, respectively. The specific capacitance was 26 F/g, when only the total activated carbon mass in the device was taken into account. The difference in the capacitances per geometrical area is most likely a result of dissimilar thicknesses of the activated carbon.

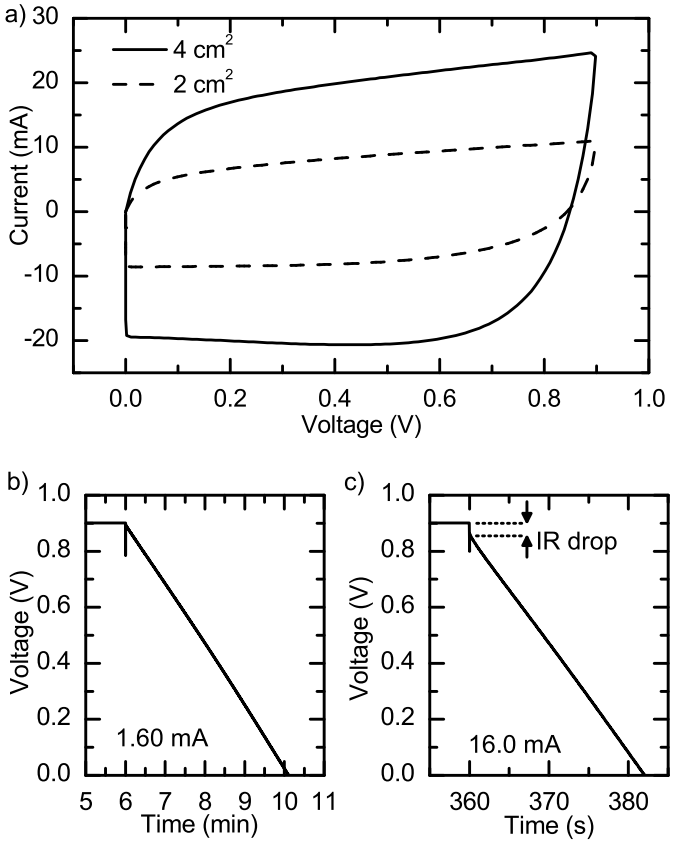

Figure 3: a) Cyclic voltammograms of two supercapacitors of different sizes. The sweep rate was 50 mV/s. b) and c) Galvanostatic discharge curves of the 4 cm^2 supercapacitor at constant discharge currents for a) capacitance determination and b) ESR determination. The ESR is calculated from the initial IR drop of the discharge. The small downward spikes at the beginning of discharge are caused by parasitic capacitances in the measurement system and not related to supercapacitor behaviour.

As expected, the ESR was larger for the smaller supercapacitors, at most 10 Ω, whereas for the larger samples it was less than 4 Ω. The larger ESR can be understood as both a resistance in the current collector leads, which were narrower in the 2 cm^2 supercapacitors, as well as a smaller cross-sectional area of the electrolyte and the separator, which inhibit the movement of current-carrying ions.

3.2. Charging the supercapacitor with the harvester

At the 5.5 cm position, the input signal to the rectifier was 20 V peak-to-peak when only the rectifier and the 10X measurement probe were connected to the antenna. At 6.0 cm, the input signal was 15 V peak-to-peak, measured similarly. These values refer to the high and low input cases discussed in below. The rectifier output DC mean values in these two cases were 4.5 V and 3.2 V in the high and low input cases, respectively.

The charging behaviour of the supercapacitors is shown in Fig. 4. In the high input case, the charging was faster; 11 min and 22 min for the 2 cm^2 and 4 cm^2 supercapacitors, respectively. With the low input, the charging took 1 h 4 min for the

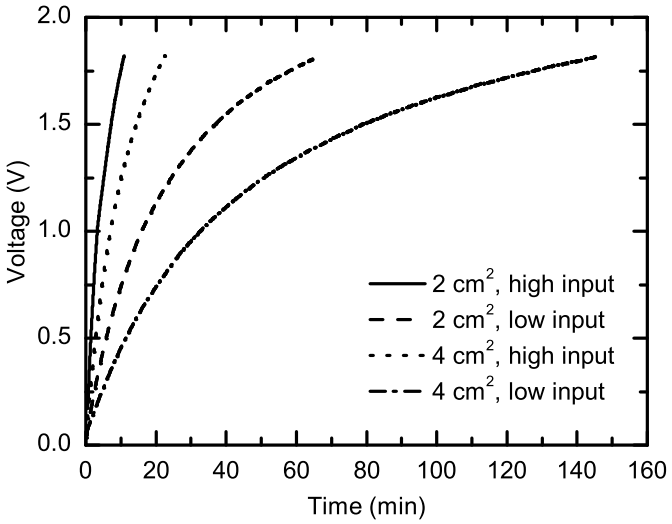

Figure 4: Charging curves to 1.8 V for the two supercapacitors connected in series.

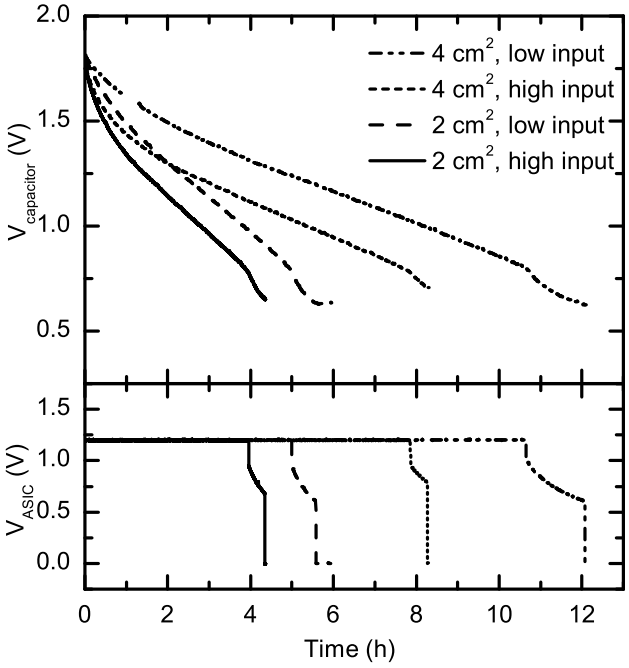

Figure 5: Voltage over the supercapacitors (above) as it powers the regulator ASIC, and the output voltage from the ASIC (below).

smaller supercapacitors and 2 h 21 min for the larger supercapacitors.

As expected, capacitance affects the charging time: a larger supercapacitor accommodates more charge and thus the required time is longer with a similar input. Ideally, the charging time for a capacitor with double the area would be twice as long; this is observed here, particularly with the high input charging curves.

A significant difference is seen between the high and low input cases, i.e. depending on the strength of the inductive coupling between the reader and harvester. The rectifier output voltages are not the same as measured without the supercapacitors: when the supercapacitors are connected to the harvester, the DC voltage at the output of the rectifier is equal to the voltage of the supercapacitor assembly, and thus dependent on its charge state. Instead, the output current of the diode determines the charging rate.

3.3. Powering the regulator circuit

The voltage over the supercapacitors when they are discharged, as well as the output voltage of the ASIC, are presented in Fig. 5. The regulator output remains constant at 1.2 V, corresponding to an output current of 1.2 μA and output power of 1.44 μW, until the voltage over the supercapacitors reaches approximately 0.78 V. The durations of operation are summarized in Table 1.

As expected, the larger, 4 cm^2 supercapacitors can power the chip for a longer time, from 8 h to over 10 h, whereas the 2 cm^2 supercapacitors can only provide the necessary input to the ASIC for 4 to 5 hours. The supercapacitor voltage behaviour is very interesting in terms of the cycle duration. In the quickly charged ("high input") supercapacitors, the initial voltage drop is much more pronounced. In the slowly charged supercapacitors ("low input"), the overall voltage decline is more uniform even in the beginning. The difference between the differently charged supercapacitors after 1 hour of discharge is approximately 0.15 V with both supercapacitor sizes.

An explanation to the observed behaviour is found in an equivalent circuit model [16], where the supercapacitor is represented as at least three parallel branches of capacitors and series resistances, each with a different RC time constant, along with another leakage resistance branch. When the supercapacitor is charged quickly, only the small-time constant branches are truly charged full; as the external charging is stopped, charge redistribution from the high time constant branches to the lower ones takes place within the supercapacitor. This results in a quick initial decrease in the observed voltage over the supercapacitor. When the supercapacitor is charged slowly, however, the slower branches are also charged full, resulting in a more steady voltage decrease as power is drawn from the supercapacitor.

In a more qualitative way, the behaviour can be understood in terms of ion migration in the supercapacitor: parts of the electrode surface, namely those deep inside the pores, are not readily accessible to the ions of the electrolyte and thus cannot initially participate in the double layer formation. However, given enough time, the ions also migrate to these surfaces. The migration can occur from the already-charged surfaces, near the pore opening, after the supercapacitor is charged externally for only a short period. This corresponds to the charge reorganization in the branched equivalent model.

4. Conclusions

Printable supercapacitors were demonstrated as energy storage devices in a harvester circuit using a printed RF antenna and

Table 1: The results of the supercapacitor characterization and harvesting measurements. High and low input refer to cases where the harvester antenna was closer to and further away from the reader antenna.

device area	4 cm^2		2 cm^2	
C (F)	0.45	0.46	0.21	0.22
C/A (0.11 F/cm^2)	0.11	0.11	0.10	0.11
ESR (Ω)	2.8	3.7	6.2	10
high input charge t	22 min		11 min	
low input charge t	2 h 21 min		1 h 4 min	
high input operation t	10 h 39 min		4 h 59 min	
low input operation t	7 h 51 min		3 h 57 min	

diode rectifier along with a voltage regulator ASIC. The two series-connected supercapacitors can be charged to 1.8 V in a time ranging from 10 minutes to over two hours, depending on the supercapacitor size and antenna distance. The output from the voltage regulator was found to stay constant at 1.2 V for up to 5 or 10 hours, depending on supercapacitor size. The results are summarized in Table 1.

The charging time, controlled by the antenna distance, was found to affect the discharge behaviour of the supercapacitor significantly. Slowly charged supercapacitors provided a more steady and long-lasting input for the regulator. The relatively rapid initial drop of the voltage in quickly charged supercapacitors is attributed to charge reorganization within the electrode pores. This important effect will need to be considered in further work aiming to develop harvester structures for different applications.

5. Acknowledgements

The authors would like to acknowledge the Academy of Finland for its financial support.

References

[1] Mathuna CO, O'Donnell T, Martinez-Catala RV, Rohan J, OFlynn B. Energy scavenging for long-term deployable wireless sensor networks. Talanta 2008;75(3):613–23.

[2] Vullers R, van Schaijk R, Doms I, Van Hoof C, Mertens R. Micropower energy harvesting. Solid-State Electronics 2009;53(7):684–93.

[3] Philipose M, Smith JR, Jiang B, Mamishev A, Roy S, Sundara-Rajan K. Battery-free wireless identification and sensing. Pervasive Computing, IEEE 2005;4(1):37–45.

[4] Ko SH, Pan H, Grigoropoulos CP, Luscombe CK, Fréchet JM, Poulikakos D. All-inkjet-printed flexible electronics fabrication on a polymer substrate by low-temperature high-resolution selective laser sintering of metal nanoparticles. Nanotechnology 2007;18(34):345202–.

[5] Forrest SR. The path to ubiquitous and low-cost organic electronic appliances on plastic. Nature 2004;428(6986):911–8.

[6] Cao Q, Zhu ZT, Lemaitre MG, Xia MG, Shim M, Rogers JA. Transparent flexible organic thin-film transistors that use printed single-walled carbon nanotube electrodes. Applied physics letters 2006;88(11):113511–.

[7] Kötz R, Carlen M. Principles and applications of electrochemical capacitors. Electrochimica Acta 2000;45(15):2483–98.

[8] Pandolfo A, Hollenkamp A. Carbon properties and their role in supercapacitors. Journal of Power Sources 2006;157(1):11–27.

[9] Keskinen J, Sivonen E, Jussila S, Bergelin M, Johansson M, Vaari A, et al. Printed supercapacitors on paperboard substrate. Electrochimica Acta 2012;.

[10] Li M, Heljo P, Lupo D. Organic diodes for energy harvesting. Proc LOPE-C 2010;.

[11] Kalanti A, Yuücetas M, Salomaa J, Aaltonen L, Halonen K. Charge-pump based frequency regulator for precision supply generation. In: Circuits and Systems (ISCAS), Proceedings of 2010 IEEE International Symposium on. IEEE; 2010, p. 4077–80.

[12] Lilja KE, Bäcklund TG, Lupo D, Hassinen T, Joutsenoja T. Gravure printed organic rectifying diodes operating at high frequencies. Organic Electronics 2009;10(5):1011–4.

[13] Pell W, Conway B, Marincic N. Analysis of non-uniform charge/discharge and rate effects in porous carbon capacitors containing suboptimal electrolyte concentrations. Journal of electroanalytical chemistry 2000;491(1):9–21.

[14] International standard: Fixed electric double layer capacitors for use in electronic equipment. iec 62391-1. 2006.

[15] Conway BE. Electrochemical Supercapacitors: Scientific Fundamentals and Applications. New York: Kluwer Academic / Plenum Publishers; 1999.

[16] Merrett GV, Weddell AS. Supercapacitor leakage in energy-harvesting sensor nodes: Fact or fiction? In: Networked Sensing Systems (INSS), 2012 Ninth International Conference on. IEEE; 2012, p. 1–5.